

# Spinon deconfinement in doped frustrated quantum antiferromagnets

Didier Poilblanc,<sup>1,2</sup> Andreas Läuchli,<sup>3</sup> Matthieu Mambrini,<sup>1</sup> and Frédéric Mila<sup>2</sup>

<sup>1</sup> *Laboratoire de Physique Théorique, Université Paul Sabatier, F-31062 Toulouse, France*

<sup>2</sup> *Institute of Theoretical Physics, Ecole Polytechnique Fédérale de Lausanne, BSP 720, CH-1015 Lausanne, Switzerland*

<sup>3</sup> *Institut Romand de Recherche Numérique en Physique des Matériaux (IRRMA), PPH-Ecublens, CH-1015 Lausanne*

(Dated: November 29, 2018)

The confinement of a spinon liberated by doping two-dimensional frustrated quantum antiferromagnets with a non-magnetic impurity or a mobile hole is investigated. For a static vacancy, an intermediate behavior between complete deconfinement (kagome) and strong confinement (checkerboard) is identified in the  $J_1-J_2-J_3$  model on the square lattice, with the emergence of two length scales, a spinon confinement length *larger* than the magnetic correlation length. For mobile holes, this translates into an extended spinon-holon boundstate allowing one to bridge momentum (ARPES spectral function) and real space (STM) experimental observations. These features provide clear evidence for a nearby "deconfined critical point" in a doped microscopic model.

PACS numbers: 75.10.-b, 75.10.Jm, 75.40.Mg

The search for exotic spin liquids (SL) has been enormously amplified after the discovery of the high critical temperature (high- $T_C$ ) cuprate superconductors. Indeed, Anderson suggested that the Resonating Valence Bond state is the relevant insulating parent state that would become immediately superconducting under hole doping [1]. Such a state is characterized by short range magnetic correlations and no continuous (spin) or discrete (lattice) broken symmetry. Another major characteristic of this SL phase is the deconfinement [2] of the  $S=1/2$  excitations (spinons) in contrast to ordered magnets which have  $S=1$  spin waves. Upon doping, some scenarios predict a 2D Luttinger liquid [3], i.e. a state which exhibits spin-charge separation, a feature generic of one-dimensional correlated conductors.

Magnetic frustration is believed to be the major tool to drive a two-dimensional (2D) quantum antiferromagnet (AF) into exotic quantum disordered phases. The Valence Bond Solid (VBS), an alternative class of quantum disordered phases breaking lattice symmetry, seems to be a strong candidate in some frustrated quantum magnets as suggested by robust field theoretical arguments [4], early numerical computations of frustrated quantum AF on the square lattice with diagonal bonds [5, 6, 7] and in the 2D checkerboard lattice [8] (with diagonal bonds only on half of the plaquettes). In contrast, the 2D kagome lattice [9] shows no sign of ordering of any kind [10, 11]. The "deconfined critical point" (DCP), a new class of quantum criticality, was proposed recently e.g. to describe a *continuous* AF to VBS transition [12].

Investigation of hole doping in frustrated magnets [13] has revealed striking differences between VBS and SL phases although they both exhibit a finite spin-spin correlation length  $\xi_{AF}$ . Viewing these phases as fluctuating singlet backgrounds, removing an electron at a given site (e.g. by chemical substitution with an inert atom) or, as in Angular Resolved Photoemission Spectroscopy (ARPES) experiments, in a Bloch state of given momen-

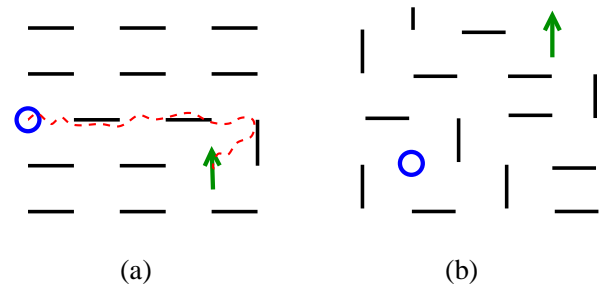


FIG. 1: (Color on-line) Schematic picture of a vacancy (or doped hole) in a frustrated magnet. The segments stand for singlet bonds and the arrow represents the spinon liberated in the process. (a) Holon-spinon BS in a columnar VBS bound by a "string" potential (dotted line). (b) Deconfined holon and spinon in an (hypothetical) SL host.

tum naturally breaks a spin dimer and liberates a spinon, i.e. a  $S=1/2$  polarisation in the vicinity of the empty site (holon). The single hole spectral function shows a sharp peak (resp. a broad feature) characteristic of a holon-spinon boundstate (resp. holon-spinon scattering states) in the checkerboard VBS phase (resp. kagome SL phase). The simple physical pictures behind these two typical behaviors are depicted in Fig. 1(a) and (b) for a confining columnar dimer phase and a SL phase respectively. The new length scale  $\xi_{\text{conf}}$  (average distance between vacancy and spinon) which emerges naturally in the VBS phase is to be identified with the correlation length over which dimer (or VBS) order sets in. Interestingly, it has been predicted that, in the vicinity of the DCP, confinement occurs on a much larger length scale  $\xi_{\text{conf}}$  which diverges as a power law of  $\xi_{AF}$  [12].

So far the DCP scenario is only supported by field theoretic arguments. It is therefore of crucial importance to investigate its relevance in the framework of microscopic models. In this Letter, we address the issues depicted in Fig. 1 by considering a single hole introduced in the 2D

spin-1/2 AF  $J_1$ - $J_2$ - $J_3$  Heisenberg model on the square lattice at zero temperature defined by

$$H = \sum_{\langle ij \rangle} J_{ij} \mathbf{S}_i \cdot \mathbf{S}_j \quad (1)$$

where the  $J_{ij}$  exchange parameters are limited to first ( $J_1$ ), second ( $J_2$ ) and third ( $J_3$ ) N.N. AF couplings. The classical phase diagram of this model [14, 15] is very rich (see Fig. 2) showing four ordered states – Néel, collinear ( $\mathbf{q} = (\pi, 0)$ ) and two helicoidal – separated by continuous or discontinuous boundaries. The subtle interplay between quantum fluctuations and frustration ( $J_2$  and  $J_3$  terms) is expected to destabilize the classical phases and lead to a quantum disordered singlet ground state, possibly of VBS type. We show that one of the major prediction of the DCP scenario, namely the emergence of a hierarchy of length scales is indeed observed for intermediate frustration in correlation with the possibility of a direct Néel-VBS continuous transition. This finding is contrasted to two other extreme behaviors -complete deconfinement and strong confinement- observed in the kagome and checkerboard lattices respectively.

Let us first briefly review some results in the literature supporting the existence of a cristaline quantum disordered phase in model (1) (leading to spinon confinement). In the parameter range where frustration is largest, many approaches, including spin-wave theory [16], exact diagonalizations [5], series-expansion [17] and large- $N$  expansions [2], have firmly established for  $J_3 = 0$  the relative stability of a quantum disordered singlet ground state: a columnar valence bond solid with both translational and rotational broken symmetries [4] or a plaquette state with no broken rotational symmetry [6] have been proposed. For the pure  $J_1 - J_3$  model, a non-classical phase also appears between the Néel  $(\pi, \pi)$  and the spiral  $(q, q)$  phases : a VBS columnar state [18] or a succession of a VBS and  $Z_2$  spin-liquid phases [19] have been proposed. Lastly, when  $J_2$  and  $J_3$  are both non-zero, in the range  $(J_3 + J_2)/J_1 \sim 0.4 - 0.6$ , the finite size scaling analysis of the dimer susceptibility computed up to 50 sites [20] shows a non-vanishing signal again strongly suggesting a VBS order [7].

A static vacancy at a given site  $O$  of the lattice is a simple setup relevant to test the DCP ideas and to experiments. In practice, the vacancy is simply modelled by setting to zero all the couplings  $J_{ij}$  involving site  $O$  and the computations are performed by Lanczos ED of a cluster of 32 sites (i.e.  $\sqrt{32} \times \sqrt{32}$ ) which respects all point group symmetries of the infinite lattice. Such an impurity acts, theoretically, as a local probe of the host. It can be viewed alternatively as a localized holon ( $S = 0$  and charge  $Q = e$ ) so that the form of the surrounding spin density is expected to provide valuable insights on the spin-charge confinement/deconfinement mechanism.

The single impurity Green function  $G(\omega) = \langle \Psi_{\text{bare}} | (\omega - H)^{-1} | \Psi_{\text{bare}} \rangle$  is computed by (i) constructing

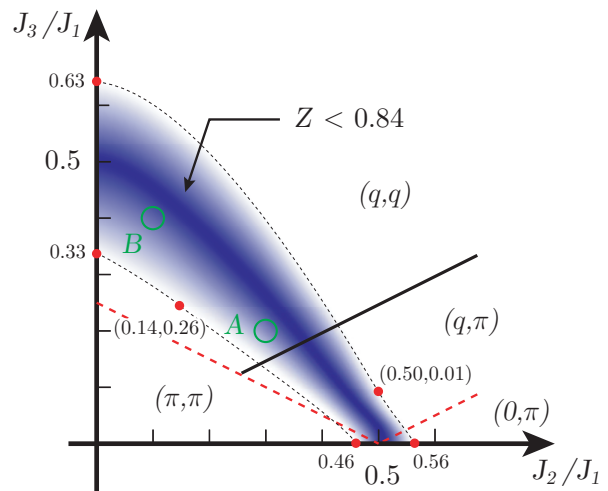


FIG. 2: (Color on-line) Classical phase diagram for the  $J_1$ - $J_2$ - $J_3$  model. Second order (discontinuous) transitions are indicated by dashed (solid) lines (see e.g. Ref. [15]). The shaded (blue online) region shows the approximate location of the minimum of the spectral weight  $Z$  in the quantum version. The region with a weight between 0.79 and 0.84 on the 32-site cluster is delimited by dashed lines and red dots.

the (normalized) "bare" initial state  $|\Psi_{\text{bare}}\rangle = 2c_{O,\sigma}|\Psi_0\rangle$  from the host GS  $|\Psi_0\rangle$  by removing an electron of spin  $\sigma$  and (ii) using a standard Lanczos continued-fraction technique. Most of the  $\omega$ -integrated spectral weight (normalized to 1) of  $\text{Im}G(\omega)$  is in fact contained in the lowest energy pole of weight  $Z = |\langle \Psi_{\text{gs}} | \Psi_{\text{bare}} \rangle|^2$  where  $|\Psi_{\text{gs}}\rangle$  is the (normalized) GS of the system with one vacancy at site  $O$ . Results shown in Fig. 3(a,b) show however that  $Z$  is significantly suppressed in the region where a quantum disordered state is expected. We show in Fig. 2 the region corresponding to a reduced weight on the 32-site cluster.

The reduction of  $Z$  is the first signal that the spinon *moves away* from the original site next to the vacancy at an average distance  $\xi_{\text{conf}}$  to be determined. A quantitative measure of this effect is provided by a careful inspection of the average local spin density  $\langle S_i^z \rangle$  around the vacancy in both the "bare" wavefunction and the true GS. Note that  $\langle S_i^z \rangle$  in  $|\Psi_{\text{bare}}\rangle$  gives the initial spin-spin correlation  $\langle S_O^z S_i^z \rangle_0$  in the host GS. We start this analysis by examining the two extreme behaviors provided by the Heisenberg model on the checkerboard and the kagome lattices reported in Fig. 4(a) and (b) respectively. Clearly, the results for the checkerboard lattice show very short-ranged and incommensurate spin-spin correlations. In addition the spinon remains almost entirely confined on the N.N. site of the vacancy. In contrast, on the kagome lattice, the spin-1/2 delocalizes on the whole lattice, a clear signature of deconfinement. Results for the  $J_1$ - $J_2$ - $J_3$  model in Fig. 5(a,b) for parameters corresponding to the two typical A and B points of the

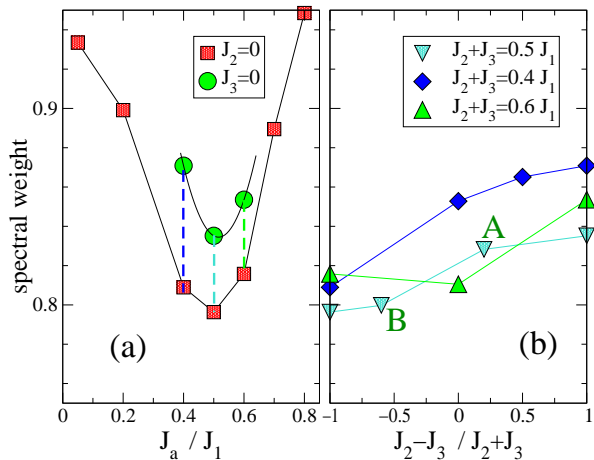


FIG. 3: (Color on-line) Static hole (vacancy) spectral weight vs AF exchange parameters. (a) vs  $J_2/J_1$  for  $J_3 = 0$  and vs  $J_3/J_1$  (for  $J_2 = 0$ ) as indicated on plot. (b) Along three different lines ( $J_2 + J_3$ )/ $J_1 = \text{cst}$  in the 2D ( $J_2/J_1, J_3/J_1$ ) parameter space. A and B refer to the points in the phase diagram of Fig. 2.

phase diagram of Fig. 2 (chosen because of a reduced  $Z$  factor) reveal completely new behaviors. First, we observe for both A and B very short magnetic correlation lengths characterized by a fast oscillating decay (with the AF wavevector) of the correlations (see below). Note that no sign of incommensurability is seen in the oscillations of Fig. 5(a) unlike in the classical spiral phase. Interestingly, the behavior of  $\langle S_i^z \rangle$  in the "relaxed"  $|\Psi_{\text{gs}}\rangle$  state differs drastically from the bare state with a *much slower decay with distance* [21]. As seen in Fig. 5, accurate fits can be realized by assuming a simple exponential decay together with an oscillatory behavior at wavevector  $(\pi, \pi)$  [22]. The very short correlation length  $\xi_{\text{AF}}$ , below one lattice spacing, is to be contrasted with the strikingly large *confinement* length  $\xi_{\text{conf}}$  typically ranging from 2 to 6 lattice spacings [23].

Let us now discuss some of the important implications of such findings. First, we note that such non-trivial extended spin structure could be seen experimentally. Indeed, the substitution of a  $S=1/2$  atom by a non-magnetic one (e.g.  $\text{Zn}^{2+}$  for  $\text{Cu}^{2+}$ ) which acts as a vacant site can be exactly described by our previous model. Moreover, the local spin densities  $\langle S_i^z \rangle$  on the magnetic sites around a vacancy (spinless atom) *in the bulk* can be directly accessed by Nuclear Magnetic Resonance (NMR). It is important to notice that NMR would probe the spinon "wavefunction" in the "relaxed" state and not the host spin correlations. Note that newly developed spin-polarized Scanning Tunneling Microscopy (SP-STM) techniques might also allow to probe such atomic-scale spin structure [24] around a vacancy *on a surface*. Secondly, at the theoretical level, the numerical evidence for a clear hierarchy of length scales,  $\xi_{\text{conf}} \gg \xi_{\text{AF}}$  provides a strong argument in favor of the

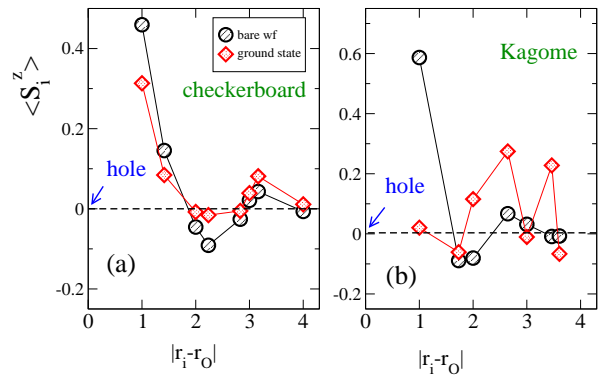


FIG. 4: (Color on-line) Spin polarization in the vicinity of the vacancy (summed up on equivalent sites) for both the "bare" vacancy state and the GS for (a) the checkerboard lattice (32 site cluster) and (b) the kagome lattice (30 site cluster).

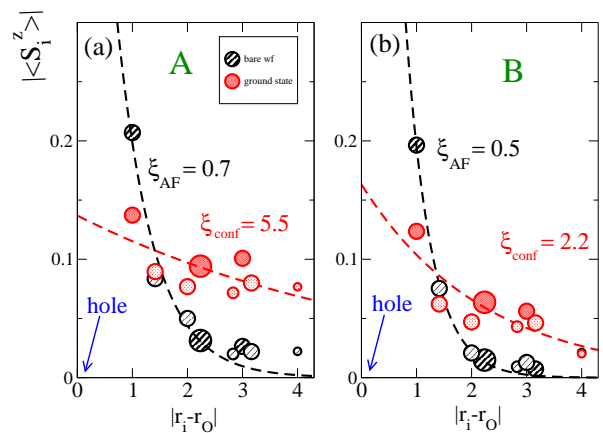


FIG. 5: (Color on-line) Same as Fig. 5 (but for the *modulus*) for the  $J_1$ - $J_2$ - $J_3$  model with  $J_2/J_1 = 0.3$  and  $J_3/J_1 = 0.2$  (a) and  $J_2/J_1 = 0.1$  and  $J_3/J_1 = 0.4$  (b) corresponding to points A and B in the phase diagram of Fig. 2. Fits using exponential forms are shown in dashed lines. The areas of the dots are proportional to the number of equivalent sites from the vacancy (entering in the fits). Dark and light symbols correspond to positive and negative values respectively.

new class of DCP [12]. Incidentally, as seen in Fig. 2, it is quite plausible that A and B lie indeed in the vicinity of the (supposed) Néel to VBS phase transition line, the paradigm of the DCP.

Lastly, we examine the case of a mobile hole. This mimics an ARPES experiment in a Mott insulator where a single photo-induced hole is created or the case of a small chemical doping. The hole motion described as in a  $t$ - $J$  model is characterized by a hole hopping amplitude  $t$ . For the unfrustrated  $t$ - $J$  model, the hole dynamics has been successfully analyzed in term of holon-spinon boundstate [25]. Note that adding motion to the hole charge leads alone to a large reduction of  $Z$ , e.g. from 0.93 ( $t = 0$ ) down to 0.36 ( $J_1/t = 0.4$ ) at small frustration ( $J_3/J_1 = 0.05$ ). As seen in Fig. 6, as frustration

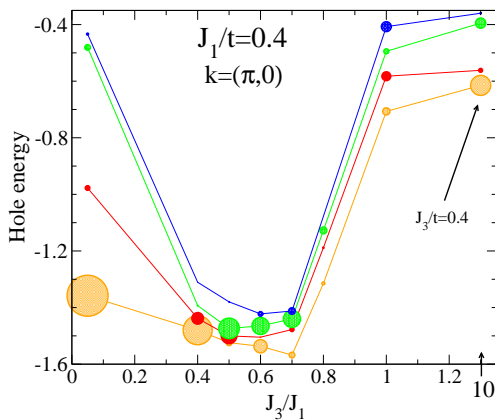


FIG. 6: (Color on-line) Four lowest energy poles of the single hole Green function (for hole momentum  $\mathbf{k} = (\pi, 0)$ ) vs increasing frustration  $J_3/J_1$ . The GS energy of the undoped AF sets the energy reference. We assume here  $J_2 = 0$  and a fixed ratio of  $J_1/t = 0.4$  ( $J_3/t = 0.4$ ) for  $J_3 \leq J_1$  ( $J_3 > J_1$ ). The areas of dots are proportional to the spectral weights  $|\langle \Psi_{\text{hole}}^{(n)} | \Psi_{\text{bare}} \rangle|^2$ ,  $n = 1, \dots, 4$ . To set the scale,  $Z \simeq 0.04$  ( $n = 1$ ) for  $J_3 = 0.6$ .

is increased, (i) the low-energy spectral weight decreases further and (ii) the quasiparticle peak (at the bottom of the spectrum) is rapidly redistributed on several poles. This remarkable behavior indicates a severe weakening of the binding between the two constituents or, equivalently, a rapid increase of the size of the holon-spinon boundstate. A spectral weight  $Z$  below 0.01 is typical in this maximally frustrated region (e.g.  $Z \simeq 0.008$  for  $J_3/J_1 = 0.5$ ). The dynamic hole problem being in fact smoothly connected to the case of a static hole [26], our data at finite  $t$  bring then additional strong evidence for the proximity of a DCP.

To conclude, the confinement of a spinon liberated by introducing a vacant site or a mobile hole has been studied in various frustrated Heisenberg AF. In the region of large frustration of the  $J_1-J_2-J_3$  model, an intermediate behavior between a strong confinement (as in the checkerboard Heisenberg model) and a complete deconfinement (as on the kagome lattice) is observed, suggesting the emergence of a new length scale related to the confinement of the spinon. Its large value compared to the spin-spin correlation length supports the field-theoretic "deconfined critical point" scenario [12] for the Néel-VBS transition. Furthermore, an interesting connection between this real-space picture and features in the hole spectral function is established.

We thank IDRIS (Orsay, France) for allocation of CPU-time on the NEC-SX5 supercomputer. D.P. acknowledges the Institute for Theoretical Physics (EPFL, Switzerland) for partial support. This work was supported by the Swiss National Fund and by MaNEP.

- 58, 2790-2793 (1987).
- [2] N. Read and S. Sachdev, Phys. Rev. Lett. **66**, 1773 (1991).
- [3] P.W. Anderson, Phys. Rev. Lett. **64**, 1839 (1990).
- [4] N. Read and S. Sachdev, Phys. Rev. Lett. **62**, 1694 (1989).
- [5] E. Dagotto and A. Moreo Phys. Rev. Lett. **63**, 2148 (1989); D. Poilblanc, E. Gagliano, S. Bacci, and E. Dagotto Phys. Rev. B **43**, 10970 (1991); H.J. Schulz, T. Ziman and D. Poilblanc, J. Phys. I (France) **6**, 675 (1996).
- [6] A plaquette phase preserving lattice *rotation* symmetry has also been proposed; see M.E. Zhitomirsky and K. Ueda, Phys. Rev. B **54**, 9007 (1996).
- [7] Note that *both* columnar and plaquette phases are picked up by the dimer "susceptibility" studied in [5].
- [8] J.-B. Fouet, M. Mambrini, P. Sindzingre, and C. Lhuillier, Phys. Rev. B **67**, 054411 (2003); see also S.E. Palmer and J.T. Chalker, Phys. Rev. B **64**, 94412 (2001).
- [9] V. Elser, Phys. Rev. Lett. **62**, 2405 (1989); P.W. Leung and V. Elser, Phys. Rev. B **47**, 5459 (1993).
- [10] P. Lecheminant et al., Phys. Rev. B **56**, 2521 (1997).
- [11] F. Mila, Phys. Rev. Lett. **81**, 2356 (1998); see also V. Subrahmanyam, Phys. Rev. B **52**, 1133 (1995).
- [12] T. Senthil et al., Science **303**, 1490 (2004); T. Senthil et al., J. Phys. Soc. Jpn. **74**, 1 (2005) and references therein.
- [13] A. Läuchli and D. Poilblanc, Phys. Rev. Lett. **92**, 236404 (2004).
- [14] A. Moreo, E. Dagotto, Th. Jolicoeur and J. Rivera, Phys. Rev. B **42**, 6283 (1990); A. Chubukov, Phys. Rev. B **44**, 392 (1991).
- [15] J. Ferrer, Phys. Rev. B **47**, 8769 (1993).
- [16] P. Chandra and B. Douçot, Phys. Rev. B **38**, R9335 (1988).
- [17] M.P. Gelfand, R.R.P. Singh and D.A. Huse, Phys. Rev. B **40**, 10801 (1989).
- [18] P.W. Leung and N.W. Lam, Phys. Rev. B **53**, 2213 (1996).
- [19] L. Capriotti and S. Sachdev, Phys. Rev. Lett. **93**, 257206 (2004).
- [20] Details about this calculation using a basis of nearest neighbor dimer coverings will be published elsewhere. See also M. Mambrini and F. Mila, Eur. Phys. J. B **17**, 651 (2000); S. Dommange, M. Mambrini, B. Normand and F. Mila, Phys. Rev. B **68**, 224416 (2003).
- [21] In contrast to the case of the unfrustrated Heisenberg antiferromagnet, the spin density *decreases* on the four nearest neighbor sites of the vacancy. See N. Bulut, D. Hone, D.J. Scalapino and E.Y. Loh, Phys. Rev. Lett. **62**, 2192 (1989).
- [22] The incommensurability seen in Fig. 5(b) at long distances does not affect the fit accuracy.
- [23] A crude fit  $\xi_{\text{conf}} = a(\xi_{\text{AF}})^\alpha$  gives  $\alpha \sim 2.5-3$ .
- [24] S. Heinze et al., Science **288**, 1805 (2000).
- [25] P. Béran, D. Poilblanc and R.B. Laughlin, Nucl. Phys. B **473**, 707 (1996) and references therein.
- [26] In the context of a  $O(3)$  field theory, a formal mapping was established (one-loop RG); see S. Sachdev, M. Troyer and M. Vojta, Phys. Rev. Lett. **86**, 2617 (2001).